Nature Environment and Pollution Technology
An International Quarterly Scientific Journal

ISSN: 0972-6268	Vol. 13	No. 3	pp. 491-498	2014

Original Research Paper

Retrieval of Leaf Area Index of Winter Wheat at Different Growth Stages Using Continuous Wavelet Analysis

Qingkong Cai, Jinbao Jiang, Ximin Cui and Liangliang Tao*(**)
College of Geoscience and Surveying Engineering, China University of Mining & Technology, Beijing 100083, China
*State Key Laboratory of Earth Surface Processes and Resource Ecology, Beijing Normal University, Beijing 100875, China
**Key Laboratory of Environmental Change and Natural Disaster, Beijing Normal University, Beijing 100875, China
Corresponding author: Jinbao Jiang

Nat. Env. & Poll. Tech.
Website: www.neptjournal.com

Received: 14-7-2014
Accepted: 14-8-2014

Key Words:
Leaf area index
Continuous wavelet analysis
Winter wheat
Hyperspectral remote sensing
Agricultural ecological environment

ABSTRACT

Leaf area index (LAI) is one of the most basic parameters to characterize the vegetation canopy structure, and is widely used in monitoring crop growth, yield estimation and other fields. Therefore, accurate estimation of LAI has great significance for agricultural precision fertilization and protecting agricultural ecological environment. However, few studies have attempted to estimate LAI of winter wheat using the continuous wavelet analysis (CWA), particularly at different growth stages. This paper aims at studying the spectral estimation of LAI by applying CWA into canopy spectra of 190 samples observed at Guanzhong Plain in China. Two partial least square regression (PLSR) models using six wavelet features and the optimal spectral indices were constructed and compared respectively. Results indicated that the model using wavelet features combination had a considerable improvement than the spectral indices combination for the whole validation dataset. When the validation dataset was separated according to the growth stage, the predictive performance of the wavelet features combination performed well at both growth stages, while the spectral indices combination had not achieved the same effect. The results showed that CWA approach could derive more robust wavelet features to growth stage variation, and wavelet features were more effective than the spectral indices for predicting LAI of winter wheat at different growth stages.

INTRODUCTION

Leaf area index (LAI) is defined as a projected green leaf area per unit ground surface area (Watson 1947, Chen & Black 1992). It is one of the key variables used by crop physiologists and modellers for estimating foliage cover, as well as monitoring and forecasting crop growth, biomass production and yield (Dorigo et al. 2007, Casa et al. 2012). Therefore, accurate monitor of LAI is of great significance for the precise agriculture fertilization, which can effectively avoid the gradual decline of ecological environment caused by the excessive inputs of chemical fertilizer.

Several approaches have been proposed to estimate LAI using remote sensing technology. Essentially, these retrieval approaches can be classified into two groups (Le Maire et al. 2008, Zheng & Moskal 2009). (i) Empirical retrieval methods, which typically consist of relating the biophysical parameter of interest against spectral data through linear or nonlinear algorithmic techniques (Broge & Mortensen 2002, Verrelst et al. 2012). Due to the simple application and data process, vegetation indices (VIs) are widely used for monitoring various crop biophysical parameters (Hatfield & Prueger 2010). However, this method strongly depends on canopy structure, leaf biochemical properties, vegetation type and soil background (Jacquemoud et al. 1996), so it is difficult to design a vegetation index applicable to all conditions. (ii) Physically-based retrieval methods, which describe the transfer and interaction of radiation inside the canopy based on physical laws and provides an explicit connection between the biophysical variables and the canopy reflectance (Li & Strahler 1986, Propastin & Erasmi 2010). They have the well-founded physical basis and higher retrieval accuracy (Jacquemoud et al. 2000). However, these methods are computationally intensive and also need many input parameters, meanwhile, some parameters are difficult to obtain, which limits the widespread application (Combal et al. 2002). Therefore, some new spectral analytical technologies need to be developed.

Recently, continuous wavelet analysis (CWA) is emerging as a promising technology in spectroscopy for deriving biochemical constituent from vegetation reflectance spectra (Blackburn 2007, Cheng et al. 2011). It has the merit of decomposing the spectra data into a number of scales that can capture useful spectral information (Luo et al. 2013,

Cheng et al. 2014). Several studies have already demonstrated the benefits of CWA for vegetation classification (Henry et al. 2004, Koger et al. 2003), quantifying leaf water content with a wider variety of species (Cheng et al. 2011, Cheng et al. 2012), quantifying leaf chlorophyll concentration (Blackburn & Ferwerda 2008) and estimating canopy water content using the airborne imaging spectroscopy data (Cheng et al. 2014). However, as we understand, few studies have attempted to estimate LAI of winter wheat using the CWA, particularly at different growth stages. Therefore, a research on the estimation of winter wheat LAI by using CWA method to extract spectral information still needed to be studied.

The study focuses on the retrieval of LAI by using CWA method to the canopy spectra of 190 winter wheat samples at two different growth stages and tests the robustness of the wavelet features to growth stage variation. We sought to answer two questions: (1) What are the optimal wavelet features (at particular scales and positions) that provide the greatest sensitivity to LAI? (2) Does the CWA approach outperform the traditional spectral index approach to estimate LAI?

MATERIALS AND METHODS

Study area: The study area (34°16' N, 108°04' E) is located at the Yangling National Agricultural Demonstration Zone of Shannxi province, China. It is situated at the centre of the Guanzhong Plain, which is one of the most important farmland areas and a key national base for agricultural products in China. It covers an area of 34000 square kilometres, with the average elevation of 500 m. It has a monsoon climate with a hot summer and a cool winter, the mean annual temperature is 12.9°C, and the mean annual precipitation is 635.1 mm with marked seasonal variations (Xu & Gao 2014). During the crop growth period from November to June next year, winter wheat is the main crop types in the area (Shun et al. 2013).

Two field measurements were conducted at the growth cycle of winter wheat in 2013, one at the jointing stage from March 31 to April 1, 2013, the other at the grain filling stage from May 27 to May 28, 2013. Juliang, Xinglin and Rougu are selected as the three core experiment sites in Yangling. Sample sites were selected at the areas that the soil and canopy conditions were fairly homogeneous on scales of tens of meters. The coordinate of each sample site was recorded on the ground with a handheld differential Global Positioning System (GPS) (Trimble 332, USA). The winter wheat canopy spectral and LAI were collected at each sample site. After removing the missing data and the abnormal data, 190 valid samples were collected at the two experiments, among them 76 in jointing stage and 114 in grain filling stage. At each stage, samples were split into two parts, half of the samples were used for models calibration, and the remaining samples were used for models validation.

Canopy hyperspectral measurements: Canopy spectra were collected in clear sky conditions by using ASD Fieldspec FR spectrometer (ASD, Boulder, USA) between 10:00 a.m. and 14:00 p.m. in local time (GMT+8). The circular probe was kept around 0.5 m vertically above the canopy. Before the canopy spectra were collected, the instrument was optimized and calibrated with a white panel (99% reflectance). In order to reduce the effect of instrument noise to the spectrum measurement, canopy spectra were measured 10 times at each sample site.

LAI measurements: The winter wheat LAI was measured with a LAI-2000 (LI-COR, Lincoln, NE) plant canopy analyser, which compares the above and below canopy light levels detected in five conical rings to infer LAI and characteristics of canopy architecture (Welles & Norman 1991). When measurements were conducted, the sun was kept behind the operator and a 45° cap was used on the LAI-2000 in order to avoid the effect of direct sunlight. For each sample, an above-canopy reading and four below-canopy recordings were collected for LAI calculation, the data were programmed to average four observations into a single LAI at each site.

Preprocessing and normalization of spectral reflectance data: To eliminate the noise effect in the data, firstly, the spectral data were smoothed by using a weighted mean moving average over a 5 nm sample (Savitzky & Golay 1964). It was found that this method gave the reflectance data sufficient smoothing without loss of fine spectral detail information (Smith et al. 2005). Due to the effect of strong absorption by water vapour and weak spectral signal, we selected 350~950 nm band that have a higher signal noise ratio as the effective analysis data. In order to suppress the possible difference of the illumination, we normalized all the spectral curves by dividing the mean band reflectance of the curve (Yu et al. 1999), the benefit of normalization by eliminating spectral difference caused by the change of illumination conditions had been demonstrated by Yu (Yu et al. 1999).

Continuous wavelet transform (CWT): Wavelet analysis is a promising method for processing hyperspectral signatures and has been successfully applied to remote sensing image processing to extract information from various scales (Simhadri et al. 1998). The CWT can decompose a signal at a continuum of positions, and the outputs from CWT are more easily interpretable. In our paper, we used CWT to

Table 1: Definitions of spectral indices involved in this paper.

Spectral indices	*Acronym*	*Formula*	*Sourse*
Ratio vegetation index	RVI	R_{800}/R_{670}	Baret et al. (1991)
Normalized difference vegetation index	NDVI	$(R_{800}-R_{670})/(R_{800}+R_{670})$	Rouse et al. (1974)
Green normalized difference vegetation index	GNDVI	$(R_{800}-R_{550})/(R_{800}+R_{550})$	Gitelson et al. (1996)
Triangle vegetation index	TVI	$60(R_{800}-R_{550})-100(R_{670}-R_{550})$	Broge et al. (2001)
Optimization of soil-adjusted vegetation index	OSAVI	$(R_{800}-R_{670})/(R_{800}-R_{670}+0.16)$	Rondeaux et al. (1996)
Modified soil-adjusted vegetation index	MSAVI	$\frac{1}{2}\left[2R_{800}+1-\sqrt{(2R_{800}+1)^2-8(R_{800}-R_{670})}\right]$	Qi et al. (1994)
Enhanced vegetation index	EVI	$2.5(R_{800}-R_{670})/(R_{800}-6R_{670}-7.5R_{485}+1)$	Liu et al. (1995)
2-bands enhanced vegetation index	EVI2	$2.5(R_{800}-R_{670})/(R_{800}+2.4R_{670}+1)$	Jiang et al. (2008)
Modified nonlinear vegetation index	MNLI	$1.5(R_{800}^2-R_{550})/(R_{800}^2+R_{670}+0.5)$	Gong et al. (2003)
Modified simple ratio	MSR	$(R_{800}/R_{670}-1)/\sqrt{(R_{800}/R_{670}+1)}$	Chen (1996)
Modified second triangular vegetation index	MTVI2	$\frac{1.5[1.2(R_{800}-R_{550})-2.5(R_{670}-R_{550})]}{\sqrt{(2R_{800}+1)^2-(6R_{800}-5\sqrt{R_{670}})-0.5}}$	Haboudanea et al. (2004)
Three gradient difference vegetation index	TGDVI	$\frac{R_{800}-R_{670}}{\lambda_{800}-\lambda_{670}}-\frac{R_{670}-R_{550}}{\lambda_{670}-\lambda_{550}}$	Tang et al.2003

Notes: here R_λ is reflectance at wavelength λ.

extract spectral information for the estimation of LAI.

CWT is a linear operation that uses a mother wavelet function to convert a hyperspectral reflectance spectrum into sets of coefficients at various scales. The main equations are as below (Cheng et al. 2014, Bruce et al. 2001).

$$\psi_{a,b}(\lambda)=\frac{1}{\sqrt{a}}\psi\left(\frac{\lambda-b}{a}\right) \quad ...(1)$$

$$W_f(a,b)=\left\langle f,\psi_{a,b}\right\rangle=\int_{-\infty}^{+\infty}f(\lambda)\psi_{a,b}(\lambda)d_\lambda \quad ...(2)$$

Where, a and b represent the scaling and shifting factor, respectively. $f(\lambda)$ (λ=1, 2 , … , n is the number of spectral bands and herein n = 601) is the reflectance spectrum. $W_f(a_i,b_j)$ (i=1, 2,…, m , j=1,2,…,n) is the output of CWT coefficients. The CWT coefficients constitute a 2-dimensional scalogram, in which one dimension is scale and the other is wavelength. Previous studies have shown that the shape of absorption features of vegetation was similar to a Gaussian or quasi-Gaussian function (Torrence & Compo 1998). So the second derivative of Gaussian (DOG) was used as the mother wavelet basis (Cheng et al. 2011, 2014, Torrence et al. 1998). In this paper, there were only 601 spectral bands available, any scale greater than 2^9=512 was discarded, because the wavelet power at higher scales did not carry meaningful information.

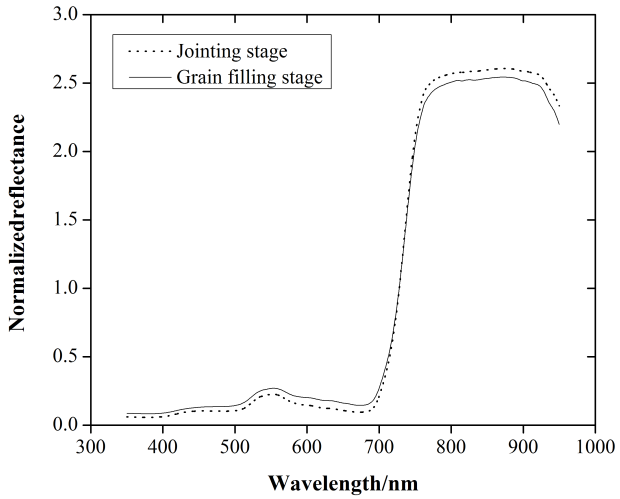

Fig. 1: Mean reflectance spectra at jointing stage and grain filling stage.

Selection of wavelet features: Among the large amount of wavelet features, the most significant ones were selected by using the strategies put forward by Cheng (Cheng et al.

Table 2: Descriptive statistics of LAI at two growth stages in 2013.

Growth period	Samples	Mean ± s.d.	Min	Max	Variation coefficient
Jointing stage	76	3.50±0.94	1.51	6.27	0.268
Grain filling stage	114	4.74±0.90	2.47	6.73	0.189
Two growth stages	190	4.24±1.10	1.51	6.73	0.259

Table 3: Coefficients of determination between LAI and spectral indices obtained from the calibration data (n=95).

Spectral indices	Model type	R^2	RMSE	Spectral indices	Model type	R^2	RMSE
RVI	Qua	0.28***	0.96	NDVI	Exp	0.32***	0.97
GNDVI	Pow	0.33***	0.99	TVI	Pow	0.21***	1.07
OSAVI	Exp	0.32***	0.97	MSAVI	Exp	0.33***	0.97
EVI	Exp	0.34***	0.95	EVI2	Pow	0.32***	0.97
MNLI	Exp	0.33***	0.96	MSR	Qua	0.31***	0.94
MTVI2	Exp	0.30***	0.99	TGDVI	Exp	0.33***	0.96
Multivariate	PLSR	0.57***	0.75				

Notes: Qua, Exp, Pow are models of quadratic, exponential and power respectively. Significance is: *p < 0.05, **p < 0.01, ***p < 0.001

2014). The Pearson's linear correlations were calculated between the wavelet power at each feature location and LAI through calibration samples, then sorted the squared correlation coefficient (R^2) in the descending order. A cut-off percentage threshold was applied to delineate the top 1% features that correlated with LAI (Cheng et al. 2011, 2014, Luo et al. 2013). These features formed a number of scattered feature regions. The feature with the maximum R^2 within each region was selected as the optimal wavelet features and expressed as (wavelength in nm, scale).

Calculation of spectral indices: Four types of spectral indices were used to compare with wavelet features, including the simple ratio and difference vegetation index: Ratio vegetation index (RVI), Normalized difference vegetation index (NDVI), Green normalized difference vegetation index (GNDVI) and Triangle vegetation index (TVI). Vegetation index that control soil influence: Optimization of soil-adjusted vegetation index (OSAVI) and the Modified soil-adjusted vegetation index (MSAVI); the increased atmospheric correction factor vegetation index: Enhanced vegetation index (EVI) and 2-bands enhanced vegetation index (EVI2); the modified vegetation index: Modified nonlinear vegetation index (MNLI), Modified simple ratio (MSR), Modified second triangular vegetation index (MTVI2) and Three gradient difference vegetation index (TGDVI), which led to a total of 12 spectral indices as given in Table 1. All these spectral indices were tested in this paper.

RESULTS AND DISCUSSION

Variation of the LAI and spectral response in different growth stages: Table 2 is the descriptive statistics of LAI at two growth stages in 2013. The range of LAI was from 1.51 to 6.27 m^2/m^2 at jointing stage and 2.47 to 6.73 m^2/m^2 at grain filling stage. The jointing stage LAI had a higher variation coefficient (26.8%) than the grain filling stage LAI (18.9%). The average normalized reflectance of winter wheat at the two different growth stages are shown in Figure 1, from jointing stage to grain filling stage, the reflectance in the visible (350~729 nm) regions increased and decreased in the NIR (729~950 nm) regions.

Estimating LAI by using the spectral indices across the datasets: A correlation analysis was calculated between the four kinds of spectral indices and LAI. Both single and multiple spectral indices were examined to calibrate the predictive model. The model performance was assessed by using the coefficient of determination (R^2) and the root mean square error (RMSE). Table 3 summarizes the R^2, RMSE, and significance level for each spectral index. All the 12 spectral indices passed the *t*-test and were significantly correlated with LAI ($P < 0.001$), with the R^2 from 0.21 to 0.34. After removing the non-significant spectral indices ($p > 0.05$) in the multiple linear regression model, the nine optimal spectral features were determined which were RVI, GNDVI, MSR, EVI, MTVI2, EVI2, MNLI, TGDVI and TVI, and the PLSR model combining with nine spectral indices were constructed. Here, we defined this model as PLSR model 1. As given in Table 3, this model demonstrated a better accuracy with a R^2 of 0.57 and a RMSE of 0.75 m^2/m^2.

Estimating LAI by using the continuous wavelet analysis: Six optimal wavelet features (Table 4) related to changes in LAI were selected, and both single and multiple spectral indices were examined to calibrate the predictive model. Results indicated that all extracted features were significantly correlated with LAI ($p < 0.001$), with the R^2

Table 4: Coefficients of determination between LAI and wavelet features obtained from the calibration data (n=95).

Wavelet features	Feature location		Model type	R^2	RMSE
	Wavelength(nm)	Scale			
$WP_{447,3}$	447	3	Exp	0.46***	0.84
$WP_{520,4}$	520	4	Exp	0.60***	0.75
$WP_{804,4}$	804	4	Pow	0.54***	0.79
$WP_{810,3}$	810	3	Lin	0.52***	0.79
$WP_{842,5}$	842	5	Lin	0.48***	0.83
$WP_{902,4}$	902	4	Exp	0.50***	0.82
Multivariate			PLSR	0.70***	0.62

Notes: Exp, Pow and Lin are models of exponential, power and linear respectively. Significance is: *p < 0.05, **p < 0.01, ***p < 0.001

Table 5: Results of the two PLSR models for the whole validation dataset and different growth stages.

Spectral metrics	Two stages		Jointing stage		Grain filling stage	
	R^2	RMSE	R^2	RMSE	R^2	RMSE
Spectral indices	0.53	0.73	0.32	0.88	0.54	0.74
Wavelet features	0.68	0.60	0.61	0.64	0.56	0.61

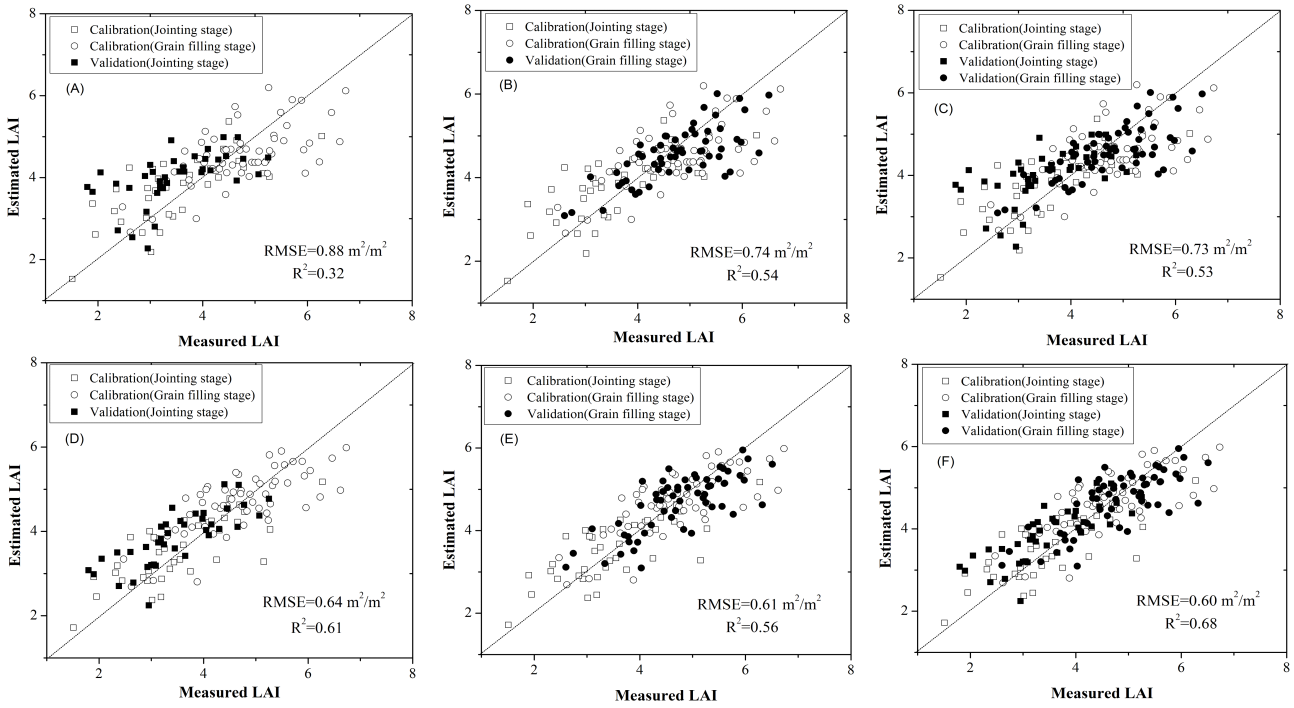

Fig. 2: Plots of measured versus estimated LAI at jointing stage (A,D), grain filling stage (B,E) and two stages (C,F), using PLSR model 1 (A,B and C) and PLSR model 2 (D,E and F). The R^2 and RMSE were obtained from the validation dataset.

ranging from 0.46 to 0.60. The maximum correlation was produced by the wavelet feature at 520 nm at scale 4 (R^2 = 0.60) and the minimum by the wavelet feature at 447 nm at scale 3 (R^2 = 0.46). Feature (520 nm, 4) occurred on the left shoulder of green peak, the green regions were identified as having the best accuracy in estimating LAI (Nguy-Robertson et al. 2014). The remaining features were all in the near-infrared spectral region, this spectral region have a stronger sensitivity to LAI and can make an efficient correction for background influences (Houborg & Eva Boegh 2008). Then

the PLSR model combining with six wavelet features were constructed and produced the best accuracy, with a R^2 of 0.70 and a RMSE of 0.62 m^2/m^2. Here, we defined this model as PLSR model 2. The R^2 showed that the wavelet features performed better than spectral indices for the estimation of LAI.

Prediction of LAI model using wavelet features and spectral indices: When applying the two PLSR models to the validation data, LAI were better predicted using PLSR model 2 than PLSR model 1 at the two growth stages (Table 5). In order to evaluate the sensitivity of LAI models to growth stage variation, the validation dataset were also divided into jointing stage data and grain filling stage data. Results indicated that the spectral metrics combination led to slightly different predictive performance between growth stages, with the predictive performance of PLSR model 2 (R^2 = 0.61 and RMSE = 0.64 m^2/m^2 at jointing stage and R^2 = 0.56 and RMSE = 0.61 m^2/m^2 at grain filling stage) and PLSR model 1 (R^2 = 0.32 and RMSE = 0.88 m^2/m^2 at jointing stage and R^2 = 0.54 and RMSE = 0.74 m^2/m^2 at grain filling stage), and model 2 exhibited substantially better performance than model 1 at jointing stage. This is mainly because the spectral signals were more easily influenced by background with a lower LAI at the jointing stage, and the CWA method had the ability to remove the effects of background spectral variation (Mittermayr et al. 2001). Moreover, the variation coefficient of LAI is relatively larger at jointing stage (26.8%) than at grain filling stage (18.9%). PLSR model 2 exhibited the similar estimation capability at the two growth stages, but PLSR model 1 had a little poorer performance at jointing stage comparing with grain filling stage, this implied that wavelet features were more robust than spectral indices to growth stage variation for estimating LAI at the two growth stages.

To make the comparison of results more visual, the scatter plots of measured versus estimated LAI are shown in Fig. 2. It was clear that PLSR model 2 made the points more convergent to the line 1:1 than PLSR model 1 for the whole validation dataset and the two growth stages, indicating that the relationship between reflectance and LAI had been improved by using the CWA method.

CONCLUSIONS

This study has demonstrated the efficiency of CWA in analysing canopy spectra and selecting features to the estimation of winter wheat LAI at two growth stages. Using the field samples from Guanzhong Plain, we extracted six wavelet features and nine optimal spectral indices, then two PLSR models based on these features were established and compared respectively. Results showed the model combining with six wavelet features (R^2 = 0.68 and RMSE = 0.60 m^2/m^2) produced promising accuracy in estimating LAI than the model combining with nine optimal spectral indices (R^2 = 0.53 and RMSE = 0.73 m^2/m^2). After partitioning the validation dataset by growth stages, predictive performance presented slight difference between growth stages. The model based on wavelet features exhibited the similar estimation capability at two stages, but the model based on spectral indices had a poorer performance at jointing stage comparing with grain filling stage, indicating that wavelet features were more robust to the growth stage variation than spectral indices for the estimation of winter wheat LAI, particularly at different growth stages.

This study extended CWA methodology to the estimation of winter wheat LAI at two different growth stages and exhibited promising results. However, problems of agricultural environmental pollution are increasingly serious due to excessive use of fertilizers. Therefore, this paper had great importance for monitoring crop growth, guiding agricultural fertilizer scientifically, protecting agricultural ecological environment and the construction of the national precision agriculture.

ACKNOWLEDGEMENTS

This work was subsidized by National Key Technology R&D Program (2012BAH29B04) and Doctoral Students Top-notch Innovative Talents Cultivation Foundation of China University of Mining & Technology Beijing (8000158656). The authors are grateful to all the staff of Beijing Normal University and Beijing Research Center for Information Technology in Agriculture for their support during field data collection.

REFERENCES

Baret, F. and Guyot, G. 1991. Potentials and limits of vegetation indices for LAI and APAR assessment. Remote Sensing of Environment, 35: 161-173.

Blackburn, G.A. and Ferwerda, J.G. 2008. Retrieval of chlorophyll concentration from leaf reflectance spectra using wavelet analysis. Remote Sensing of Environment, 112: 1614-1632.

Blackburn, G.A. 2007. Wavelet decomposition of hyperspectral data: A novel approach to quantifying pigment concentrations in vegetation. International Journal of Remote Sensing, 28: 2831-2855.

Broge, N.H. and Leblanc, E. 2001. Comparing prediction power and stability of broadband and hyperspectral vegetation indices for estimation of green leaf area index and canopy chlorophyll density. Remote Sensing of Environment, 76: 156-172.

Broge, N.H. and Mortensen, J.V. 2002. Deriving green crop area index and canopy chlorophyll density of winter wheat from spectral reflectance data. Remote Sensing of Environment, 81: 45-57.

Bruce, L.M. and Li, J. 2001. Wavelets for computationally efficient hyperspectral derivative analysis. IEEE Transactions on Geoscience and Remote Sensing, 39: 1540-1546.

Casa, R., Varella, H. and Buis, S. 2012. Forcing a wheat crop model with LAI data to access agronomic variables. Evaluation of the impact of model and LAI uncertainties and comparison with an empirical approach. European Journal of Agronomy, 37: 1-10.

Cheng, T., Riaño, D. and Ustin, S.L. 2014. Detecting diurnal and seasonal variation in canopy water content of nut tree orchards from airborne imaging spectroscopy data using continuous wavelet analysis. Remote Sensing of Environment, 143: 39-53.

Cheng, T., Rivard, B. and Sánchez-Azofeifa, G.A. 2011. Spectroscopic determination of leaf water content using continuous wavelet analysis. Remote Sensing of Environment, 115: 659-670.

Cheng, T., Rivard, B. and Sánchez-Azofeifa, G.A. 2012. Predicting leaf gravimetric water content from foliar reflectance across a range of plant species using continuous wavelet analysis. Journal of Plant Physiology, 169: 1134-1142.

Chen, J.M. and Black, T.A. 1992. Defining leaf area index for non-flat leaves. Agr. Forest Meteorol., 57: 1-12.

Chen, J.M. 1996. Evaluation of vegetation indices and modified simple ratio for boreal applications. Canadian Journal of Remote Sensing, 22: 229-242.

Combal, B., Baret, F. and Weiss, M. 2002. Retrieval of canopy biophysical variables from bidirectional reflectance using prior information to solve the ill-posed inverse problem. Remote Sensing of Environment, 84: 1-15.

Dorigo, W.A., Zurita-Milla, R. and de Wit, A.J.W. 2007. A review on reflective remote sensing and data assimilation techniques for enhanced agroecosystem modeling. International Journal of Applied Earth Observation and Geoinformation, 9: 165-193.

Gitelson, A.A., Kaufman, Y.J. and Merzlyak, M.N. 1996. Use of a green channel in remote sensing of global vegetation from EOS-MODIS. Remote Sensing of Environment, 58: 289-298.

Gong, P., Pu, R. and Biging 2003. Estimation of forest leaf area index using vegetation indices derived from Hyperion hyperspectral data. IEEE Transactions on Geoscience and Remote Sensing, 41: 1355-1362.

Haboudanea, D., Miller, J.R. and Pattey, E. 2004. Hyperspectral vegetation indices and novel algorithms for predicting green LAI of crop canopies: Modeling and validation in the context of precision agriculture. Remote Sensing of Environment, 90: 337-352.

Hatfield, J.L. and Prueger, J.H. 2010. Value of using different vegetative indices to quantify agricultural crop characteristics at different growth stages under varying management practices. Remote Sensing, 2: 562-578.

Henry, W.B., Shaw, D.R. and Reddy, K.R. 2004. Remote sensing to detect herbicide drift on crops. Weed Technology, 18: 358-368.

Houborg, R. and Eva Boegh, E. 2008. Mapping leaf chlorophyll and leaf area index using inverse and forward canopy reflectance modeling and SPOT reflectance data. Remote Sensing of Environment, 112: 186-202.

Jacquemoud, S., Bacour, C., and Poilvé, H. 2000. Comparison of four radiative transfer models to simulate plant canopies reflectance: Direct and inverse mode. Remote Sensing of Environment, 74: 471-481.

Jacquemoud, S., Ustin, S. and Verdebout, J. 1996. Estimating leaf biochemistry using the PROSPECT leaf optical properties model. Remote Sensing of Environment, 56: 194-202.

Jiang, Z.Y., Huete, A.R. and Didan, K. 2008. Development of a two-band enhanced vegetation index without a blue band. Remote Sensing of Environment, 112: 3833-3845.

Koger, C.H., Bruce, L.M. and Shaw, D.R. 2003. Wavelet analysis of hyperspectral reflectance data for detecting pitted morning glory (*Ipomoea lacunosa*) in soybean (*Glycine max*). Remote Sensing of Environment, 86: 108-119.

Le Maire, G., Francois, C. and Soudani, K. 2008. Calibration and validation of hyperspectral indices for the estimation of broadleaved forest leaf chlorophyll content leaf mass per area, leaf area index and leaf canopy biomass. Remote Sensing of Environment, 112: 3846-3864.

Liu, H.Q. and Huete, A.R. 1995. A feedback based modification of the NDVI to minimize canopy background and atmosphere noise. IEEE Transactions on Geoscience and Remote Sensing, 33: 457-465.

Li, X.W. and Strahler, A.H. 1986. Geometrical-optical modeling of a conifer forest canopy. IEEE Transactions on Geoscience and Remote Sensing, 24: 906–919.

Luo, J.H., Huang, W.J. and Yuan, L. 2013. Evaluation of spectral indices and continuous wavelet analysis to quantify aphid infestation in wheat. Precision Agriculture, 14: 151-161.

Mittermayr, C.R., Tan, H.W. and Brown, S.D. 2001. Robust calibration with respect to background variation. Applied Spectroscopy, 55: 827-833.

Nguy-Robertson, A.L., Peng, Y. and Gitelsona, A.A. 2014. Estimating green LAI in four crops: Potential of determining optimal spectral bands for a universal algorithm. Agricultural and Forest Meteorology, 192-193: 140-148.

Propastin, P. and Erasmi, S. 2010. A physically based approach to model LAI from MODIS 250 m data in a tropical region. International Journal of Applied Earth Observation and Geoinformation, 12: 47-59.

Qi, J., Chehbouni, A. and Huete, A.R. 1994. A modified soil vegetation adjusted index. Remote Sensing of Environment, 48: 119-126.

Rondeaux, G., Steven, M. and Baret, F. 1996. Optimization of soil-adjusted vegetation indices. Remote Sensing of Environment, 55: 95-107.

Rouse, J.W., Haas, R.H. and Schell, J.A. 1974. Monitoring the vernal advancements and retrogradation of natural vegetation. In: NASA/GSFC, Final Report, Greenbelt, MD, USA, pp. 1-137.

Savitzky, A. and Golay, M.J.E. 1964. Smoothing and differentiation of data by simplified least squares procedures. Analytical Chemistry, 36: 1627-1639.

Shun Sheng Wang, Liang Jun Fei and Chuan Chang Gao 2013. Experimental study on water use efficiency of winter wheat in different irrigation methods. Nature Environment & Pollution Technology, 12(1): 183-186.

Simhadri, K.K., Lyengar, S.S. and Holyer, R.J. 1998. Wavelet-based feature extraction from oceanographic images. IEEE Transactions on Geoscience and Remote Sensing, 36: 767-778.

Smith, K. L., Steven, M.D. and Colls, J.J. 2005. Plant spectral responses to gas leaks and other stresses. International Journal of Remote Sensing, 26: 4067-4081.

Tang, S.H., Zhu, Q.J. and Wang, J.D. 2003. Theoretical bases and application of three gradient difference vegetation index. Science in China: Series D, 33: 1094-1102.

Torrence, C. and Compo, G.P. 1998. A practical guide to wavelet analysis, Bulletin of the American Meteorological Society, 79: 61-78.

Verrelst, J., Muñoz, J. and Alonso, L. 2012. Machine learning regression algorithms for biophysical parameter retrieval: Opportunities for Sentinel-2 and -3. Remote Sensing of Environment, 118: 127-139.

Watson, D.J. 1947. Comparative physiological studies in the growth of field crops. I: variation in net assimilation rate and leaf area between species and varieties, and within and between years. Annals of Botany, 11: 41-76.

Welles, J.M. and Norman, J.M. 1991. Instrument for indirect measurement of canopy architecture. Agronomy Journal, 83: 818-825.

Xu, X.Q. and Gao, J.N. 2014. Water quality assessment using

multivariate statistical techniques: A case study of Yangling Section, Weihe River, China. Nature Environment & Pollution Technology, 13(2): 225-234.

Yu, B., Ostland, I.M. and Gong, P. 1999. Penalized discriminant analysis of *in situ* hyperspectral data for conifer species recognition. IEEE Transactions on Geoscience and Remote Sensing, 37: 2569-2577.

Zheng, G. and Moskal, L.M. 2009. Retrieving leaf area index (LAI) using remote sensing: Theories, methods and sensors. Sensors, 9: 2719-2745.